Mechanical Characterization and Constitutive Modeling of a Snap Cure Neat Epoxy Under Dynamic Loading

Yu Zeng[1], Duane Cronin[1], John Montesano[1]
[1] Department of Mechanical & Mechatronics Engineering, University of Waterloo, 200 University Ave. West, Waterloo, ON, N2L 3G1, Canada

Abstract

Owing to their potential energy absorption capabilities, continuous fiber-reinforced plastic (FRP) composites are more frequently considered for use in automotive structures subjected to impact loading, where understanding the inherent loading rate-dependent mechanical properties is essential to predict structural performance. The rate-dependent behavior of the polymer resin will tend to dominate the rate-dependent response of FRP composite materials containing brittle fibers, so it is important to quantify this effect for automotive crash applications. This study investigated the tensile properties of a three-part snap curing resin system formulated for rapid resin transfer molding processes over a range of strain rates (10^{-4} to 10^{2} s^{-1}). A series of tensile tests were conducted using an MTS hydraulic testing machine for static loading, and a hydraulic intermediate strain rate test frame (HISR) for intermediate loading. The experimental results revealed that both the tensile modulus and strength of the resin system increased with increasing applied strain rates. The samples exhibited limited ductile behavior at low strain rates, while a brittle response was observed at higher strain rates. Elastic-plastic constitutive models using Power-law and Johnson-Cook rate-dependent methods were investigated to predict the strain rate dependency of the tested material in a commercial finite element software (Abaqus), and the Johnson-Cook method provided an improved fit to the experimental data when compared to the Power-law method. Overall, this study provides an initial estimate of the resin strain rate effects to support the analysis of FRP for automotive crash applications.

Introduction

Given a 10% weight reduction, the fuel economy of a gasoline vehicle can improve 6%~8% without sacrificing performance, while for an electric vehicle the driving range can increase by 13.7% [1]. Carbon fiber reinforced plastics (CFRPs) may play a key role in vehicle weight reduction because of their attractive properties, e.g., high specific strength and stiffness, and resistance to fatigue failure and corrosion. However, tailoring the orthotropic properties and complex microstructures of CFRPs to suit vehicle performance requirements using accurate and robust numerical simulation methods is still a challenge for automakers [2]. During the last decade, the progress of computational power and finite element software have given support to the multiscale modeling approach which can be used to predict the mechanical performance of CFRPs through virtual tests. However, there is little research on characterizing and modeling the behavior of a two-phase CFRP composite material when subjected to high strain rate (i.e., dynamic) and impact loading conditions using multiscale modeling strategies [3] [4], which would otherwise be applicable for automobile structures.

The properties of CFRPs depend on the properties of the constituent materials and their interfaces, the geometry and architecture of the reinforcing phase, as well as the phase volume fractions and distribution [5] [6]. When simulating CFRPs, a multiscale modeling strategy is favorable because of the nature of the material structure, where different energy dissipation mechanics may be present at various length scales [7]. Although a broad range of multiscale

methods exists, the core concept of these approaches is to use various numerical models at different length scales to represent the material structure, including micro- scale (fiber and matrix), meso- scale (lamina) and macro-scale (whole laminate). To predict the resin-dominant strain rate-dependent response of a CFRP material using a micro-scale model, a high-fidelity resin constitutive model is critical [8].

The strain rate sensitivity of polymers is an important behavior to capture in a reliable resin constitutive model, and there are many previous studies on this topic. Buckley and Harding [9] studied three thermosetting resins in compression at the strain rate of 10^{-3} to $5 \times 10^{3}\ s^{-1}$, and all three materials exhibited a clear strain rate sensitivity. Gilat et al. [10] investigated E-862 and PR-520 resins under tensile and shear loadings at the strain rate of $5 \times 10^{-5}, 2,$ and $400 - 700\ s^{-1}$; the results showed that different loading rate affects the behaviors of both resins significantly. Clive and Jennifer [11] provided a complete review of test methods for the dynamic loading behaviors of polymers because of the strain rate sensitivity of the polymer. However, most of the previous research focuses on the epoxy resin designed for aerospace applications, where the resin curing time is not sensitive. There is little information about snap-cure epoxy systems with short curing cycle times, which are more conducive for automotive applications. Additionally, a large percentage of previous studies fabricated epoxy specimens in the laboratory, lacking connection to the industrial manufacturing process.

In this study, a snap-cure epoxy material fabricated using High-Pressure Resin Transfer Molding (HP-RTM) was characterized by a series of tensile tests at different applied strain rates, and the corresponding rate-dependent behavior was predicted using an elastic-plastic constitutive model. It presented the initial steps of developing an epoxy resin constitutive model for calibrating a multiscale model of carbon fiber/epoxy composite material, capable of accurately predicting the strain rate dependent behavior due to the impact loading environment.

Materials

A three-part fast-cure epoxy system, EPIKOTE™ 06150 (Hexion Inc), designed for mass-production of lightweight carbon fiber-reinforced epoxy structural components was investigated. The epoxy material was processed into 4mm-thick 900 mm x 550 mm solid panels using full-scale HP-RTM equipment. During the panel fabrication process, the resin, curing agent, and internal mold release were mixed at a pressure of 120 bar using a high flow injection system (KrausMaffei) with a ratio of 100:24:1.2 parts by weight, correspondingly. Then, the mixture was injected through a mixing head into a closed vacuum mold held at a constant temperature of 120°C. A 25,000 kN hydraulic press (Dieffenbacher) was used to impose a 1000 kN force on the mold during injection and a 3000 kN force during the subsequent 5 min curing cycle.

After fabrication, the epoxy panels were found to have slight curvature at the edges. Also, there was visible porosity distributed around the center section of the panel where the resin was injected into the mold. Consequently, the center portion of the panels was removed, and the curved pieces were flattened before test specimen preparation. The curved panels were softened in an air-circulated oven by applying heat in a rate of 5 °C/min from ambient temperature to 120°C, which is in the glass transition region of the material. After removal from the oven, the hot panels were placed between two heavy metal plates for flattening while they cooled to ambient temperature (Figure 1).

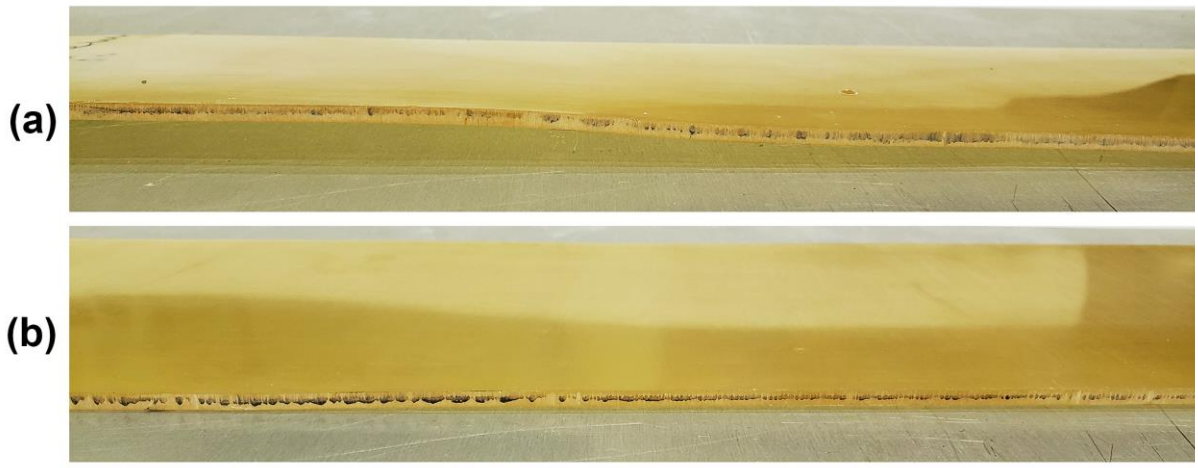

Figure 1. Fabricated neat resin panel (a) containing a curved surface after HP-RTM processing, (b) with a flat surface after flattening.

Mechanical Testing Procedures

Specimen Geometries

Modified dog-bone shaped specimens were machined from the fabricated panels and used for quasi-static and intermediate strain rate tensile tests (Figure 2). This geometry was suitable for performing tensile tests across a range of strain rates. A previous study compared the proposed geometry with that recommended by ASTM type V, and a good agreement was found between the two geometries in quasi-static tests [12]. The gauge width of the specimen used in this study was 3mm for quasi-static strain rate and 2mm for the intermediate strain rate tensile test. The DIC results showed that the major and minor strain were uniformly distributed in the gauge section of the specimens during deformation.

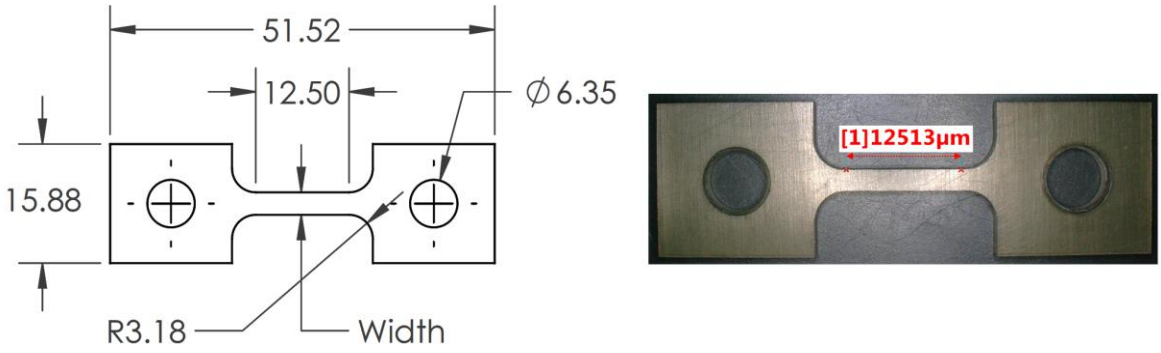

Figure 2. Modified dog-bone geometry used for tensile tests.

Test Equipment and Software

Tests were carried out in a stable temperature (24 ± 1°C) and relative humidity (50 ± 5%) lab environment. Quasi-static ($\dot{\varepsilon} \ll 0.01\ s^{-1}$) strain rate tests used a servo-hydraulic test frame with an MTS FlexTest SE controller, where the applied load was measured by an OMEGA LC412-500 load cell. Intermediate strain rate tests were conducted at a hydraulic intermediate strain rate (HISR) apparatus which functioned by accelerating an engagement sleeve to a constant velocity which then contacted the engagement piston at the bottom of the stroke. An MTS 407 control was used to control the loading process, while the applied force was measured by a KISTLER 9341B piezoelectric force sensor (Figure 3). The deformation of the specimens was measured by a digital image correlation (DIC) method. In this method, the specimens were painted with stochastic speckle pattern on the gauge section area, and the loading motions were recorded by a Nikon D3200 optical camera for quasi-static strain rate tests (1920 x 1080 pixels with 30 frames per second or fps) and a Photron SA5 high-speed camera for intermediate strain rate tests (1024 x 1024 pixels with 7000 fps, and 192 x 592 pixels with 50,000 fps).

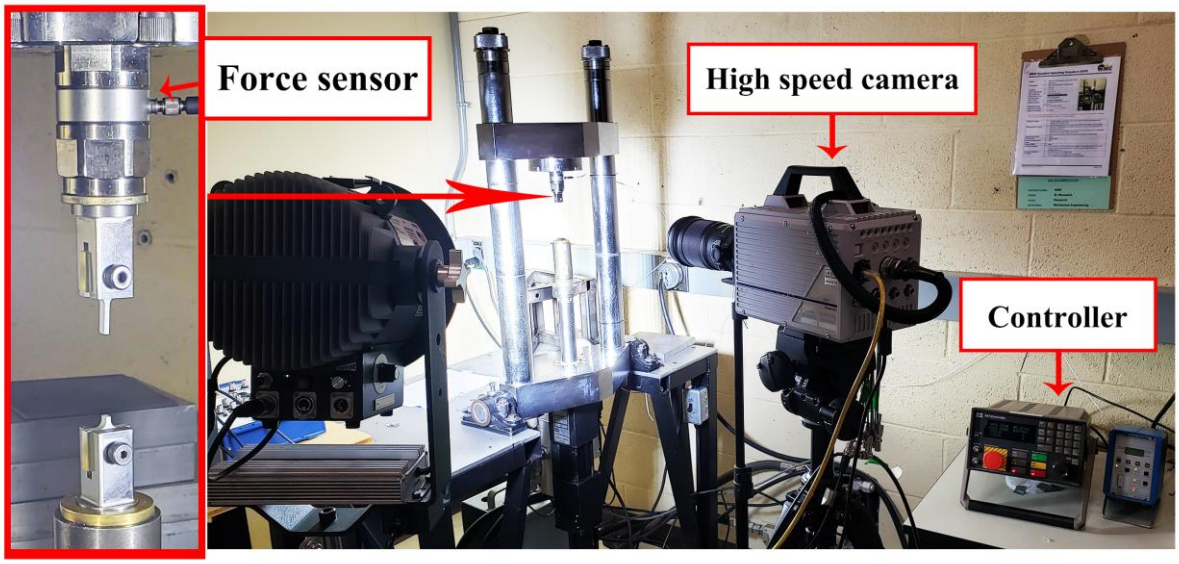

Figure 3. Intermediate strain rate tensile test setup

An industry-grade DIC software, GOM Correlate, analyzed the images to calculate the deformation of the specimens without using any strain filter. For the DIC setup, the subset sizes were 15 pixels for D3200 and 32 pixels for SA5, while the step size was determined according to the frame rate, which was one frame per step. The specimen fracture surface was then investigated with a KEYENCE optical digital microscope and a high-resolution zoom lens, VH-Z500R (500 – 5000X).

Test Setup

The tension behavior of the material was characterized at four strain rates, two quasi-statics and two intermediates. For quasi-static strain rate tests, uniaxial tensile tests were performed at a constant crosshead displacement rate (CCDR) of 0.001 and 0.01in/s. For intermediated strain rate tests, the crosshead displacement rates were set to 150mm/s and 1000mm/s. For each test condition, a minimum of five specimens was tested.

Experimental Results and Discussion

Mechanical test results

Figure 4 shows the engineering stress-strain response of the TRAC 06150 epoxy under uniaxial tensile loading at the different strain rates, which were calculated using a DIC method. From the quasi-static strain rate test results (Figure 4 (a) and (b)), the material demonstrates a limited ductile behavior, while a more brittle behavior is observed for the intermediate strain rate tests (Figure 4 (c) and (d)). Overall, the linear elastic region of the stress-strain curves is less than 2% strain. For each loading condition, good consistency of the stress-strain response between specimens that extracted from different sections of the epoxy panel is observed, which indicates the mechanical properties of TRAC 06150 epoxy are uniform and stable over the panels. The fracture strain of specimen shows notable variation, which is primarily dominated by the defects that occur during specimen manufacturing and machining processes. The tests conducted with the strain rate of 3.2 s^{-1} have notably low fracture strains compared to other strain rate tests. This situation may have been a result of the applied loading frequency which is close to the natural frequency of the hydraulic loading device, and it previously reported as a common challenge for a hydraulic intermediate strain rate apparatus [11].

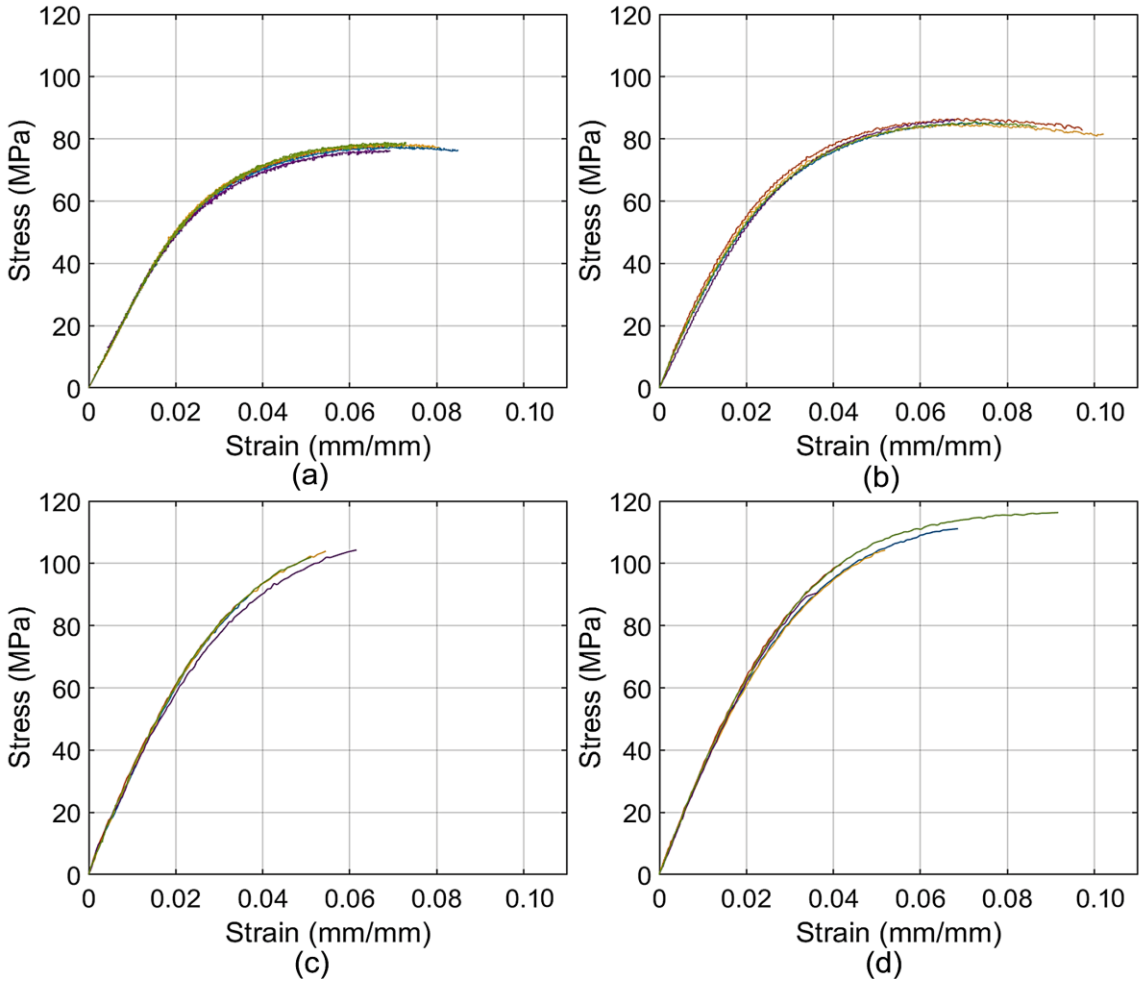

Figure 4. Engineering stress versus engineering strain curve for four tensile tests at different strain rates (five repeats for each loading condition): (a) strain rate of $3.3 \times 10^{-4}\ s^{-1}$*; (b) strain rate of* $3.5 \times 10^{-3}\ s^{-1}$*; (c) strain rate of* $3.2\ s^{-1}$*; (d) strain rate of* $23.9\ s^{-1}$

The elastic modulus, tensile strength, 0.3% offset yield strength and Poisson's ratio were carefully determined based on the stress and strain results, and a 90% confidence interval for each value was calculated using Student's t-distribution (Table 1).

Table I: Critical mechanical properties for tensile tests at different strain rates (90% confidence interval)

Strain Rate (s^{-1})	3.3×10^{-4}	3.5×10^{-3}	3.2	23.9
Elastic Modulus (GPa)	2.70 ± 0.09	3.02 ± 0.23	3.12 ± 0.12	3.25 ± 0.08
Tensile Strength (MPa)	77.6 ± 1.8	85.8 ± 1.3	97.5 ± 16.1	104.6 ± 19.4
Poisson's Ratio	0.39 ± 0.02	0.36 ± 0.04	0.38 ± 0.04	0.39 ± 0.02
Yield Strength at 0.3 % offset (MPa)	55.9 ± 3.0	53.9 ± 4.1	70.9 ± 5.3	73.4 ± 4.5

The elastic modulus was measured as the slope of the stress-strain curves between 0.1% and 1% strain, where the initial unstable data resulting from grip sliding or specimen/grip misalignment was avoided. The Poisson's ratio was calculated as the ratio of negative transverse strain rate to the axial strain rate in the elastic range, where all the strain rates were measured by the DIC method. Yield strength was determined as 0.3% strain offset of the elastic modulus slope line. It has been noticed that there were different methods to define the yield strength of a polymer, from 0.3% to 2% strain offset. In this study, a 0.3% offset was selected since it was commonly accepted in the polymer technical community [13]. As Table 1 showed, increased elastic modulus and tensile strength were associated with higher strain rates, while the Poisson's ratio remained as a constant at 0.38±0.04. For the yield strength, a notable increase presented as the strain rate increased from quasi-static to intermediate strain rate.

Fracture Surface

All the specimen fracture in a brittle manner without necking, with similar fracture pattern for all tested strain rates. This phenomenon indicates that although the stress-strain curves in Figure 4 (a) and (b) exhibit some degree of ductility, the epoxy is sufficiently brittle, and the mechanisms leading to fracture do not change with strain rate.

Figure 5 shows the typical fracture pattern of the failure specimens observed by a digital optical microscope. The crack propagation follows several well-known stages for thermosetting polymers: mirror-like, smooth with parabolas, hackle, and roughness [14]. The fracture process initiates at a local specimen defect, which can be a void or a machining mark, usually located on the surface of the specimen. After that, the crack propagates at a slow rate, creating a smooth and pattern-less surface, often call the mirror-like stage (Figure 5 A). As the crack propagation speed increases with the increase of applied stress, parabolic patterns appear due to the formation of secondary crack (Figure 5 B), referred to the smooth with parabolas stage. During the subsequent hackle stage, ellipse shape patterns are formed when the primary crack propagation speed increases, as shown in Figure 5 C. At the final roughness stage, the abrupt fracture of the specimen creates rough surfaces and complex patterns (Figure 5 D).

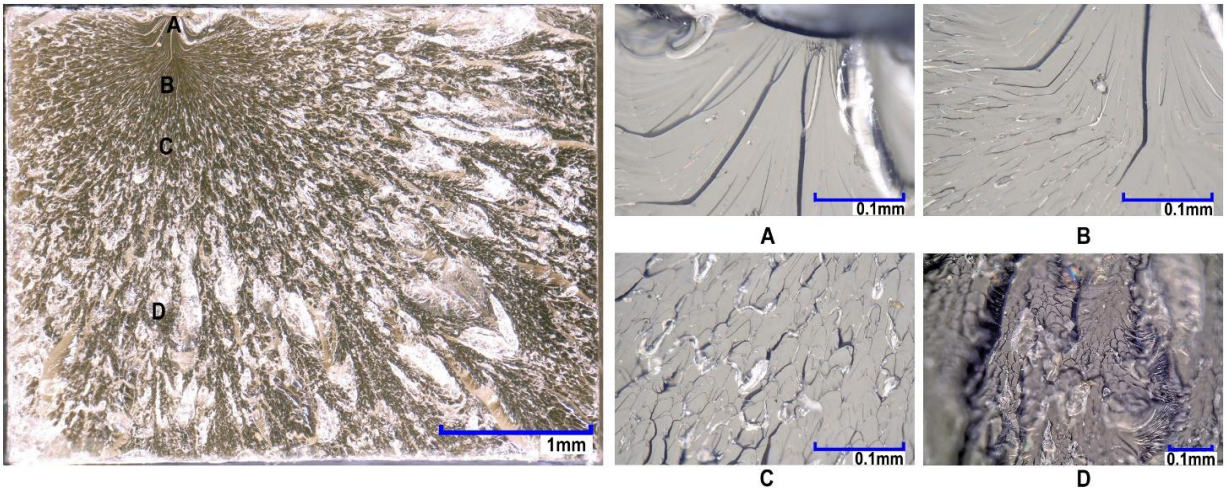

Figure 5. Fracture surface images for quasi-static strain rate test

Constitutive model

An assessment of the existing rate-dependent material models in the commercial Finite Element Analysis (FEA) software, Abaqus, was undertaken in this study. In Abaqus, polymers with strain rate-dependent response can be modeled as elastic-plastic or viscoelastic materials. The elastic-plastic constitutive model was selected because it was widely available, easy to use and numerically efficient, and it had been extensively used to describe the behavior of thermoplastic polymers [15]. Using a metal elastic-plastic model to simulate the nonlinear viscoplastic behavior of polymers may in some cases produce inaccurate predictions, especially during cyclic loading or unloading, which are not including in this dynamic loading study. A sophisticated viscosplastic model may provide an improved description of the polymer stress-strain behaviors and will be investigated in future research. For the elastic-plastic model in Abaqus, other than an experimental data tabular method, there are three methods to incorporate the rate-dependent hardening behavior: Power-Law, Yield-Ratio, and Johnson-Cook. All three methods require as input a plastic stress-strain curve from a quasi-static strain rate test to determine the stress-strain response at the higher strain rates. Furthermore, the yield ratio method shifts the inputted plastic stress-strain curve without adjusting its shape, which is not considered in this study.

The Power-Law or Cowper-Symonds overstress is a widely used method that incorporates rate dependence to a material model for commercial FEA software like Abaqus and LS_DYNA. The rate-dependent yield stress (σ_y) is calculated as:

$$\sigma_y = \sigma_y^0 \times \left(1 + \left(\frac{\dot{\varepsilon}^{pl}}{D}\right)^{\frac{1}{n}}\right) \quad (1)$$

where σ_y^0 is the true quasi-static plastic stress-strain behavior after yielding, and $\dot{\varepsilon}^{pl}$ is the corresponding plastic strain rate of yield stress, and D and n are fitting parameters.

The Johnson-Cook strain rate-dependent model assumes that the rate-dependent yield stress is defined by:

$$\sigma_y = \sigma_y^0(\mathrm{C} \cdot \ln\left(\frac{\dot{\varepsilon}^{pl}}{\dot{\varepsilon}_0^{pl}}\right) + 1) \tag{2}$$

where $\dot{\varepsilon}_0^{pl}$ is the plastic strain rate for the inputted static stress-strain behavior, and C is a fitting parameter.

The true stress-strain test data was used to provide a comparison with Power-Law and Johnson-Cook predictions. Figure 6 (A) shows the experimental true plastic stress verse true plastic strain for all strain rates considered; the blue curve that has the lowest strain rate was used as an input for Abaqus. After using a curve fitting tool (MATLAB) to determine the parameters (D, n, and C), the yield stresses for different strain rate can be determined based on inputted data, Equation (1), and Equation (2). As Figure 6 (B) shows, both Power-Law and Johnson-Cook give an excellent agreement between data and the model at the quasi-static strain rate. For the intermediate strain rates considered, both methods show reasonable correlation with the experimental data (Figure 6 (C) and (D)), albeit with a larger deviation at increasing strain rate.

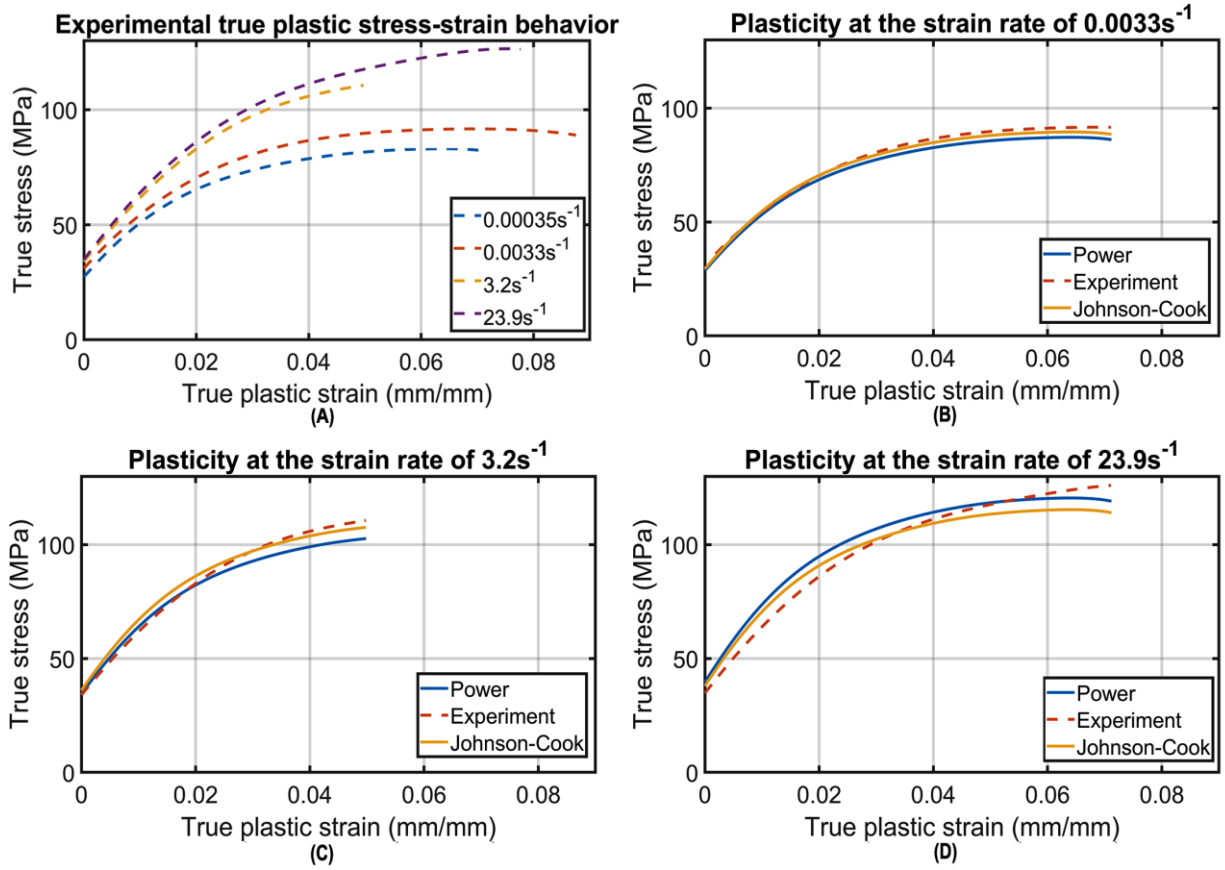

Figure 6. Power law and Johnson-Cook methods for elastic–plastic strain rate dependence

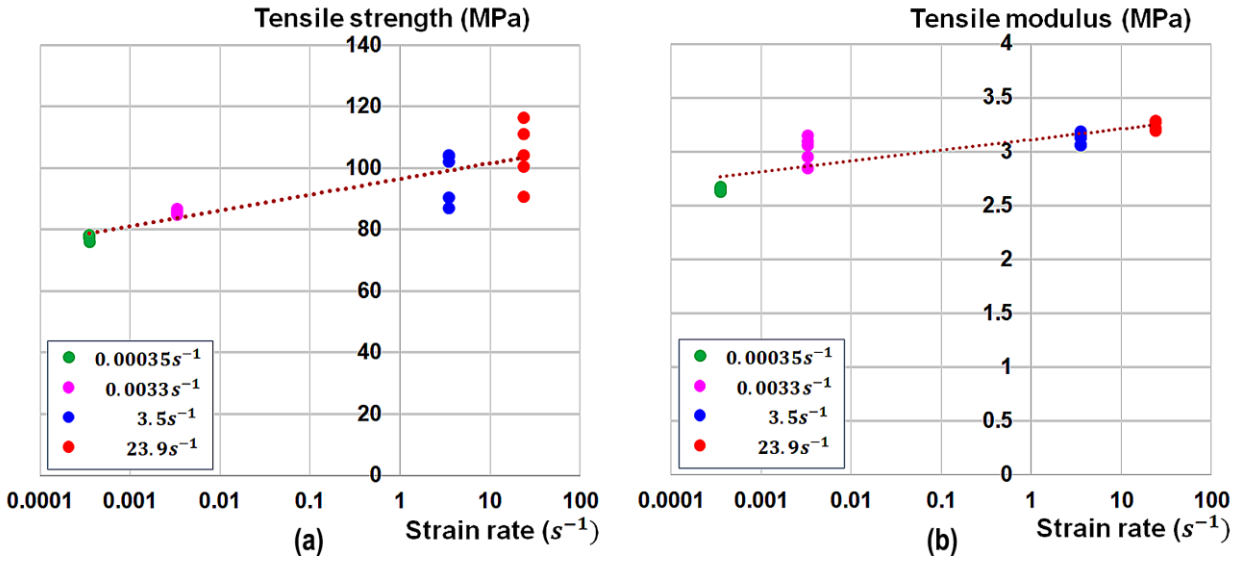

Figure 7. (a) Tensile strength verse logarithmic strain rate; (b) Tensile modulus verse logarithmic strain rate

Many materials exhibit a linear-logarithmic relation between the tensile strength and strain rates, and this is the assumption of the standard Johnson-Cook model. Figure 7 shows that the tensile strength and tensile modulus of the studied material are not in good linear-logarithm relation with the strain rates, which limits the accuracy of using the standard Johnson-Cook model to describe the strain rate dependency this epoxy. Unlike metallic materials, polymers demonstrate a nonlinear viscoplastic response, which requires additional time-dependent or frequency-dependent terms to capture the rate-dependent stress-strain behaviors accurately. Overall, the Johnson-Cook model provides a better experimental data correlation than the Power-Law model in terms of the strain rate dependency of this epoxy.

Conclusions and Future Work

In this paper, a series of tensile tests were conducted at the different applied strain rates to characterize the tensile properties of a snap curing thermosetting resin. The results showed that the resin exhibited limited ductile behavior at low strain rates, while they presented brittle response at high strain rates. A higher elastic modulus and tensile strength were associated with a higher strain rate, while the Poisson's ratio remained constant at all strain rates considered. Assessment of the fracture surface analysis revealed that the specimen fractured in a brittle manner, with similar fracture patterns at all strain rates, while the fracture processes agreed with typical fracture stages of thermosetting polymers. An elastic-plastic constitutive model incorporated with rate-dependent hardening was also investigated in Abaqus. For strain rate-dependent behaviors, Johnson-Cook method provided a better experimental data correlation than Power-Law method.

For future work, high strain rate (10^2~10^3 s^{-1}) uniaxial tensile tests will be performed using a Polymeric Split Hopkinson Tension Bar (SHTB), while compression tests and uniaxial shear tests will also be conducted at different strain rates to attain the comprehensive mechanical properties

of the studied epoxy. For constitutive modelling, the metal elastic-plastic model may not be sufficient to provide an accurate description of the polymeric material at high strain rates. A viscoplastic model, which involves developing a user-defined material model, will be considered since it may yield improved predictions. These steps will further contribute to developing a multiscale model which can accurately predict the mechanical performance of fiber-reinforced plastic composite materials.

Acknowledgements

The authors would like to thank the Natural Sciences and Engineering Research Council of Canada (NSERC) for financial support through Collaborative Research and Development Grant, as well as industrial sponsors Honda R&D Americas, Hexion Inc., Zoltek Corp. and LAVAL International. The authors also thank Luis Trimino Rincon, Brock Watson, and Tom Gawel for their help in conducting the lab experiments, while the Fraunhofer Project Center for Composites Research (London, Canada) is acknowledged for fabricating the panels.

References

1. William Joost, Reducing Vehicle Weight and Improving U.S. Energy Efficiency Using Integrated Computational Materials Engineering, JOM: the journal of the Minerals, September 2012, Volume 64, Issue 9, pp 1032–1038
2. S.R. Reid, G. Zhou, Impact Behaviour of Fibre-reinforced Composite Materials and Structures, CRC Press, Boca Raton FL Oct 31, 2000, pp.6-7
3. Young W. Kwon, David H. Allen, Ramesh Talreja, Multiscale Modeling and Simulation of Composite Materials and Structures, Springer, New York, NY, 2008
4. N. Razali, M.T.H. Sultan, F. Mustapha, N. Yidris and M.R. Ishak, Impact Damage on Composite Structures – A Review, 2014, The International Journal of Engineering and Science (IJES) Volume 3 Issue 7, Pages 08-20
5. Amos Gilat, Robert K. Goldberg, Gary D. Roberts, Strain Rate Sensitivity of Epoxy Resin in Tensile and Shear Loading, NASA Glenn Research Center; Cleveland, OH, United States, March 2005, 40p, (NASA/TM—2005-213595)
6. Isaac M. Daniel, Ori Ishai, Engineering Mechanics of Composite Materials, Second Edition, Oxford University Press, New York, NY, 2006, pp. 3-4
7. Mark E. Tuttle, Structural Analysis of Polymeric Composite Materials, Second Edition, CRC Press, New York, NY, Dec 3, 2012, Chapter 1
8. J.LLorca, C. González, J. M. Molina-Aldareguía, J. Segurado, R. Seltzer, F. Sket, M. Rodríguez, S. Sádaba, R. Muñoz, L. P. Canal, Multiscale Modeling of Composite Materials: a Roadmap Towards Virtual Testing, Adv Mater. 2011 Nov 23;23(44):5130-47
9. C.P. Buckley, J. Harding, J.P. Hou, C. Ruiz, A. Trojanowski, Deformation of thermosetting resins at impact rates of strain. Part I: Experimental study, Journal of the Mechanics and Physics of Solids 49 (2001) pp.1517 – 1538
10. Amos Gilat; Robert K. Goldberg; and Gary D. Roberts, Strain Rate Sensitivity of Epoxy Resin in Tensile and Shear Loading, JOURNAL OF AEROSPACE ENGINEERING, 2007, 20:2, pp.75-89
11. Clive R. Siviour, Jennifer L. Jordan, High Strain Rate Mechanics of Polymers: A Review, Journal of Dynamic Behavior of Materials, 2016, 2, pp.15–32
12. L.F. Trimino, D. Cronin, Evaluation of numerical methods to model structural adhesive response and failure in tension and shear loading, J. Dynamic Behavior Mater 2 (2016) 122–137.
13. M.A. Semeliss, g. Wong, M.E. Turtle, The Yield and Post-Yield Behavior High-Density Polyethylene, NASA-Langley Research Center Grant No. NAG-I-974, 1990, pp.4-6
14. Roulin-Moloney AC. Fractography and failure mechanics of polymers and composites. London: Elsevier Applied Science, 1989
15. Jörgen Bergström, Mechanics of Solid Polymers: Theory and Computational Modeling, Elsevier, San Diego, CA, 2015, pp.367-368